Journal of Asian Earth Sciences 131 (2016) 123–137

Contents lists available at ScienceDirect

Journal of Asian Earth Sciences

journal homepage: www.elsevier.com/locate/jseaes

Full length article

A detrital record of continent-continent collision in the Early-Middle Jurassic foreland sequence in the northern Yangtze foreland basin, South China

Tao Qian [a], Shaofeng Liu [b,c,*], Zongxiu Wang [a], Wangpeng Li [d], Xinlu Chen [e]

[a] Key Laboratory of Shale Oil and Gas Geological Survey, Institute of Geomechanics, Chinese Academy of Geological Science, Beijing 100081, China
[b] School of Earth Sciences and Resources, China University of Geosciences, Beijing 10083, China
[c] State Key Laboratory of Geological Processes and Mineral Resources, China University of Geosciences, Beijing 100083, China
[d] Petroleum Exploration and Production Research Institute, SINOPEC, Beijing 100083, China
[e] CNOOC Tianjin Company, Tianjin 300452, China

ARTICLE INFO

Article history:
Received 2 June 2016
Received in revised form 20 September 2016
Accepted 22 September 2016
Available online 22 September 2016

Keywords:
Northern Yangtze plate
Foreland basin
Middle Jurassic
Sediment provenance
Continent-continent collision

ABSTRACT

The Mesozoic northern Yangtze foreland basin system was formed by continental collision between the North China and South China plates along the Mianlue suture. Synorogenic stratigraphic sequences of Late Triassic to Early-Middle Jurassic age were developed in the northern Yangtze foreland basin. The upper Middle Jurassic Shaximiao Formation consists mainly of thick-bedded terrestrial successions that serve as the main body of the basin-filling sequences, suggesting intense tectonism in the peripheral orogeny of the foreland basin. Laser-ICP-MS U-Pb analysis of 254 detrital zircon grains from sandstone samples and several published Lower-Middle Jurassic samples, detrital compositions, petrofacies, and paleocurrent reconstructions in the northern Yangtze foreland basin indicate that discrete source areas included the Qinling-Dabieshan ranges and the Mianlue suture zone to the north, and the South China plate to the south. The stratigraphic succession and sediment provenance of the foreland basin imply that the early Mianlue oceanic basin, magmatic arc, and nonmarine molasse foreland basin during the period of deposition were modified or buried by the subsequent continent-continent collision between the North China-Qinling-Dabieshan plate and the Yangtze plate during the Jurassic, which followed the oblique amalgamation between these plates during the Middle-Late Triassic.

© 2016 Elsevier Ltd. All rights reserved.

1. Introduction

The Qinling-Dabieshan orogen formed during the collision between the South China and North China plates along two north-dipping suture zones in central China. These suture zones are the Shangdan suture, which developed during the Late Paleozoic, to the north, and the Mianlue suture, which formed during the Early Mesozoic, to the south (Zhang et al., 2001; Liu et al., 2005, 2015a, 2015b; Li et al., 2014) (Fig. 1). The two sutures separated three crustal fragments from north to south: the North China plate, the Qinling-Dabieshan microplate, and the South China plate, which consists of the Yangtze plate in the north and the Cathaysia plate in the south (Zhang et al., 2013; Liu et al., 2015b) (Fig. 1). Amalgamation of the Yangtze plate and the North China-Qinling-Dabieshan complex plate resulted in a continent-continent collision during the Middle to Late Triassic. It has been confirmed that the Yangtze plate started to obliquely collide with the North China-Qinling-Dabieshan complex plate since the Middle-Late Triassic (Liu et al., 2005, 2015b; Zhu et al., 2009). However, it is still unclear whether this compressional orogenesis continued after the collision of these two plates and how synorogenic units developed during the Early-Middle Jurassic, although there has been some previous research by Enkin et al. (1992), Gilder and Courtillot (1997), Yokoyama et al. (2001), and Liu et al. (2005). Long-distance subduction of the northern Yangtze plate under the Qinling-Dabieshan plate led to the destruction of parts of the northern Yangtze plate; furthermore, postorogenic erosion has removed many of the supracrustal units, thereby hampering reconstructions of the basin-mountain distribution of this area. Sedimentation into adjacent foreland basins can provide another constraint on at least the late stages of collisional deformation of the northern Yangtze plate. This information promotes our understanding of the orogen-parallel evolution of the major continental suture. Unfortunately, much of the synorogenic supracrustal units

* Corresponding author at: State Key Laboratory of Geological Processes and Mineral Resources, China University of Geosciences, Beijing 100083, China.
E-mail address: shaofeng@cugb.edu.cn (S. Liu).

http://dx.doi.org/10.1016/j.jseaes.2016.09.016
1367-9120/© 2016 Elsevier Ltd. All rights reserved.

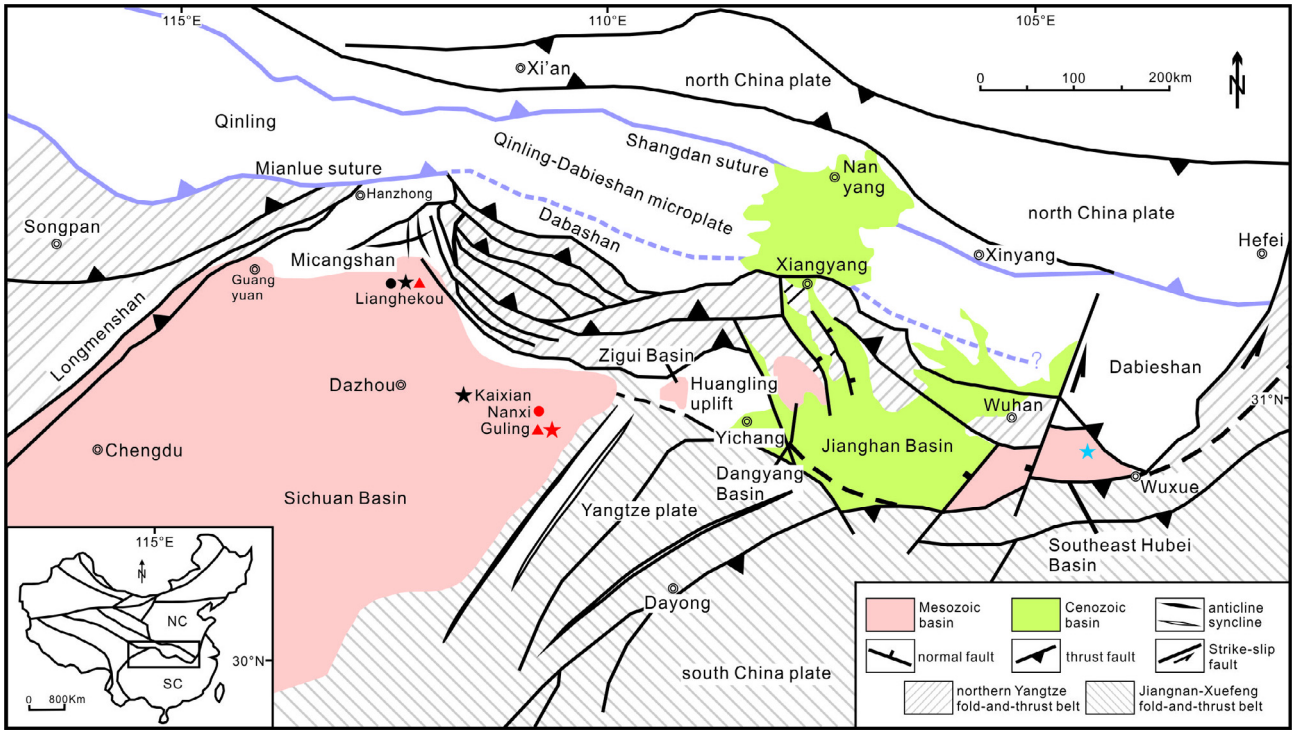

Fig. 1. Structural map of the southern Qinling-Dabie orogen and northern Yangtze plate (modified from Liu et al. (2005)). The black circle and stars denote detrital zircon sandstone samples of the Middle Jurassic Qianfoya and Shaximiao formations, respectively, cited from previous studies (Li et al., 2010; Luo et al., 2014); the blue star denote detrital zircon sample of the Middle Jurassic Huajiahu Formation of Southeast Hubei Basin (Yang et al., 2010); the red circles and stars denote detrital zircon sandstone samples obtained from the Qianfoya and Shaximiao formations, respectively, in the present study. The red triangles indicate sites of measured stratigraphic sections. (For interpretation of the references to color in this figure legend, the reader is referred to the web version of this article.)

have been eroded away; therefore, here we attempt to investigate the synorogenic units of the northern Yangtze plate and improve understanding of the collisional process between the North China-Qinling-Dabieshan and Yangtze plates during the Early-Middle Jurassic. To this end, we synthesize evidence from basin-filling sequences, petrologic constraints, paleoflow reconstructions, and detrital zircons in the foreland basin of the southern Qinling-Dabieshan fold-thrust belt. The northern Yangtze foreland basin contains thick sedimentary fills of Late Triassic to Cenozoic age. The basin provides a relatively continuous record of source-area deformation and unroofing, allowing us to infer the exhumation and denudation of the evolving source areas.

2. Tectonic setting and basin stratigraphy

The southern Qinling-Dabieshan foreland fold-thrust belt is divided into northern, southern, and frontal subbelts (Liu et al., 2015b). The southern subbelt includes the Longmenshan, the east-west striking Micangshan, and the arcuate Dabashan fold-thrust belts, which underwent orogenesis related to amalgamation of the North China-Qinling-Dabieshan and Yangtze plates. The folds and thrusts in this subbelt mainly involve Cambrian to Middle Triassic strata in the north, and Upper Triassic to Middle Jurassic foreland basin deposits in the south. The Longmenshan fold-thrust belt bounding western margin of the Sichuan Basin is defined by three NE- or SW-dipping thrust faults. This region experienced at least two major shortening events: tectonism associated with Late Triassic collision between the North China and South China plates, and deformation related to eastward growth of the Tibetan Plateau during the Mesozoic (Yan et al., 2011; Li et al., 2014). The east-west striking Micangshan fold-thrust belt is adjacent to the Dabashan to the east and the Longmenshan to the west (Fig. 1). Previous studies have demonstrated that Micangshan fold-thrust belt experienced moderate denudation during the Cenozoic (Tian et al., 2012). Rapid pre-Late Cretaceous cooling in the Micangshan fold-thrust belt was coeval with the thrusting event, which affected the deposition of sediments in the Late Jurassic to Early Cretaceous foredeep of the northwestern Yangtze plate (Liu et al., 2005, 2015b; Tian et al., 2012). The Dabashan fold-thrust belt, a typical NE-SW-protruding arcuate structure (Fig. 1), underwent NE-SW shortening during the Late Triassic to Early Jurassic in response to continental collision between the Yangtze and North China plates (Zhao and Coe, 1987; Nie et al., 1994). There is evidence that the Dabashan fold-thrust belt was thrust over the primary Micangshan fold-thrust belt; additionally, the observation that the western part of the Dabashan fold-thrust belt truncates the eastern Micangshan fold-thrust belt demonstrates that the Micangshan fold-thrust belt underwent tectonic deformation earlier than did the Dabashan fold-thrust belt.

During the Late Triassic and Early-Middle Jurassic collision-induced orogenesis, marine sedimentation in the Mianlue suture zone ceased and the Mianlue oceanic basin evolved into a peripheral foreland basin. Located in the northwestern part of the Yangtze plate, the Sichuan and Zigui basins formed as a foreland basin in which marine-nonmarine molasse was deposited during the Middle-Late Triassic. Commencing in the Early Jurassic, a thick succession of continental strata was deposited in the basin. The Lower-Middle Jurassic sequence includes the Baitianba Formation (Lower Jurassic), Qianfoya Formation (early Middle Jurassic), and Shaximiao Formation (late Middle Jurassic); these formations are well exposed in the Sichuan and Zigui basins (Fig. 2).

The Baitianba Formation occurs above an angular unconformity that separates it from the Upper Triassic Xujiahe Formation. The formation is composed of fining-upward successions beginning with a basal conglomerate featured by a meandering riverbed

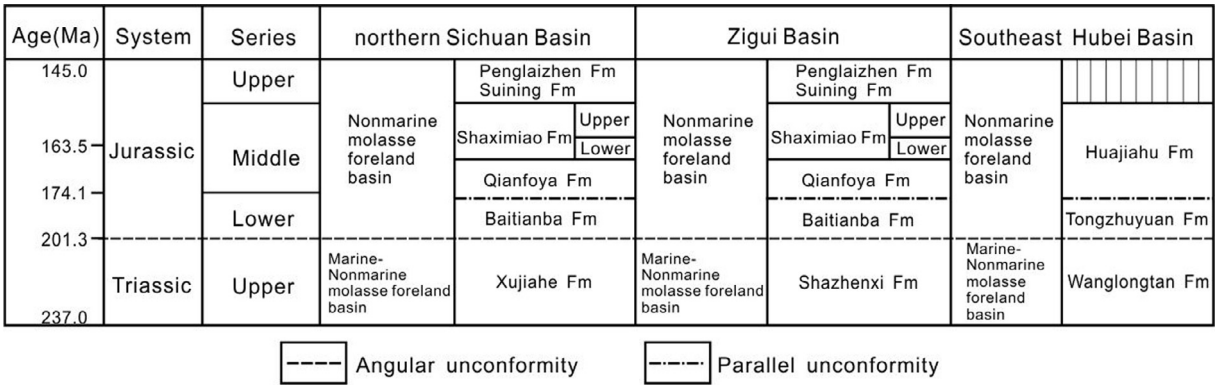

Fig. 2. Upper Triassic to Upper Jurassic stratigraphic units and their correlation across the Sichuan, Zigui and Southeast Hubei basins. Fm, Formation.

(Allen, 1978). Fine- to medium-grained sandstone and conglomeratic sandstone with massive bedding and tabular cross-bedding along with tree trunks occur above the conglomerate. Alternations of thick-bedded fine-grained sandstone, laminated siltstone, and mudstone overlie the sand bodies interlayered with thin-bedded coal layers or coal seams (Fig. 3). The lower part of the Middle Jurassic is represented by the Qianfoya Formation, which consists of fining-upward depositional cycles characterized by meandering river or shore and shallow-lacustrine successions (Fig. 3). Each cycle begins with a thin-bedded conglomerate or fine- to medium-grained sandstone with massive or tabular stratification. Upward in the cycle, the coarser sediments are capped by thick-bedded rhythmic siltstone with well-developed parallel laminations, sandy mudstone, and mudstone containing lenticular coarse-grained sandstone. Abundant leaf fragments and fossils of nonmarine bivalves are found in the finer sediments. The thick succession of the Shaximiao Formation (upper Middle Jurassic) filled most of the foreland basin. The Shaximiao Formation consists primarily of several coarsening-upward successions with localized fining-upward units containing siltstone, silty mudstone, and mudstone, as well as medium- to coarse-grained sandstone (Fig. 3). All cycles can be divided into two parts: the lower part consists of thick-bedded alternations of siltstone, silty mudstone, and mudstone with a flaser-wavy-lenticular-bedded interval containing thinly bedded fine- to medium-grained sheet sandstone; and the upper part contains conglomeratic sandstone, medium- to coarse-grained sandstone with large-scale tabular, trough, wedge, and massive cross-stratification with local sharp, undulating, scour-filling surfaces (Fig. 3). The Shaximiao Formation successions are interpreted as braided-stream delta deposits.

3. Samples and methods

3.1. Point-counting

Hand samples were collected in the field where exposure was good and the sandstone grain size was fine, medium, or coarse. Thin sections were prepared and 500–600 framework grains were counted per slide. Because of the wide range of rocks exposed in the Qinling-Dabieshan orogenic belt, lithic composition is an important and effective indicator of the source area. We used the traditional method of point-counting and plotted the results for lithic composition (Fig. 3). Although we only show the results as percentages, taking the consistency of grain size (mostly medium-grained sandstone) into consideration, we infer that lithic compositional percentages are useful as source-area indicators. We used the Gazzi-Dickinson method, which minimizes the influence of grain size, to plot the point-counting results on total quartz-feldspar-lithic (Qt-F-L), monocrystalline quartz-feldspar-total lithic (Qm-F-Lt), and polycrystalline quartz-volcanic fragments-sedimentary fragments (Qp-Lv-Ls) ternary diagrams to provide insight into the tectonic background of the source areas. Compared with the traditional method, the Gazzi-Dickinson method yields higher percentages of Q and F, and lower percentages of L.

3.2. Detrital zircon U-Pb dating

Zircons were dated in situ using a laser ablation-inductively coupled plasma-mass spectrometer (LA-ICP-MS) at the State Key Laboratory of Continental Dynamics, Northwest University, Xi'an, China. Zircons were separated by heavy-liquid and magnetic methods and purified by handpicking under a binocular microscope. More than 600 zircon grains were picked from each sample, from which a total of 120 zircons were analyzed. Cathodoluminescence (CL) images of the zircons were used to reveal the internal textures of the zircons and to select optimal spot locations for U-Pb dating. The CL images reveal the complicated structure of most detrital zircons. Most zircons exhibit clear oscillatory zoning of magmatic origin; those which with no growth rims or narrow growth rim structure are of metamorphic origin. We typically selected spots on the areas of oscillatory zoning for U-Pb dating. Alternatively, the cores were dated if the areas of zoning were extremely narrow or absent. The spot size and laser frequency were 30 μm and 10 Hz, respectively. The data acquisition mode was peak jumping (20 ms per isotope each cycle). The concentrations of U, Th, and Pb were calibrated using ^{29}Si as an internal standard and NIST 610 as the reference standard. Each analysis consisted of about 20 s of gas blank and 40 s of signal acquisition. The $^{207}Pb/^{206}Pb$, $^{206}Pb/^{238}U$, $^{207}Pb/^{235}U$, and $^{208}Pb/^{232}Th$ ratios, calculated using Glitter 4.0 (Macquarie University), were corrected for both instrumental mass bias and depth-dependent elemental and isotopic fractionation using Harvard zircon 91500 as an external standard. Age calculations and concordia diagrams were made using Isoplot 3 (Ludwig, 2003). Standard analytical details for the ages, and the trace and rare earth element determinations of the zircons were as reported in Yuan et al. (2004). Grains yielding ages with more than 10% discordance were not included in the probability density distribution curves and the final interpretation. All analytical results for concordant zircons, U-Pb ages, and Th/U ratios are provided in the Supporting Information. We used $^{207}Pb/^{206}Pb$ ages for zircons of age $\geqslant$1.0 Ga, and $^{206}Pb/^{238}U$ ages for zircons of age <1.0 Ga.

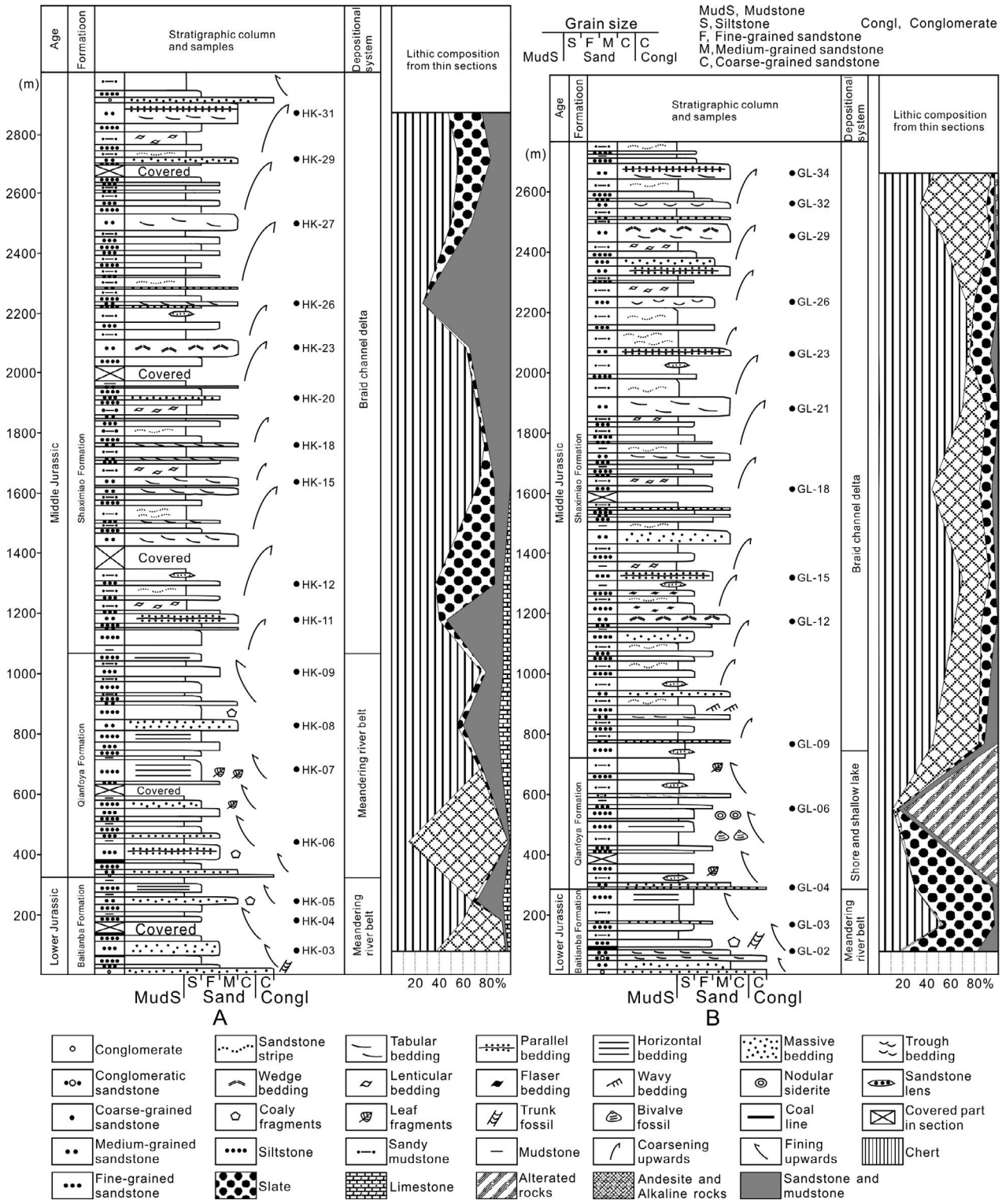

Fig. 3. Lower-Middle Jurassic stratigraphic sections near the towns of Lianghekou (A) and Guling (B), northern Sichuan Basin. The locations of the sections are marked in Fig. 1. The right-hand column of each section is a summary of lithic fragment data from thin sections of sandstone samples.

4. Ternary plots, lithic composition, and petrofacies

4.1. Ternary plots of sandstone composition, and source analyses

In general, Middle Jurassic sandstones from the northern Yangtze foreland basin are dominated by chert, andesite, and sedimentary rock fragments. Most samples fall in the field of recycled orogen provenance in Qt-F-L and Qm-F-Lt ternary diagrams (Fig. 4); some fall in the field of collision suture, fold-thrust belt, and arc-orogen sources in the Qp-Lv-Ls ternary diagram (Fig. 4). Consequently, the main source areas of the Middle Jurassic northern Yangtze foreland basin are the southern Qinling-Dabieshan foreland fold-thrust belt, the consumed island-arc belt of the Mianlue suture, and the pre-closure Mianlue ocean.

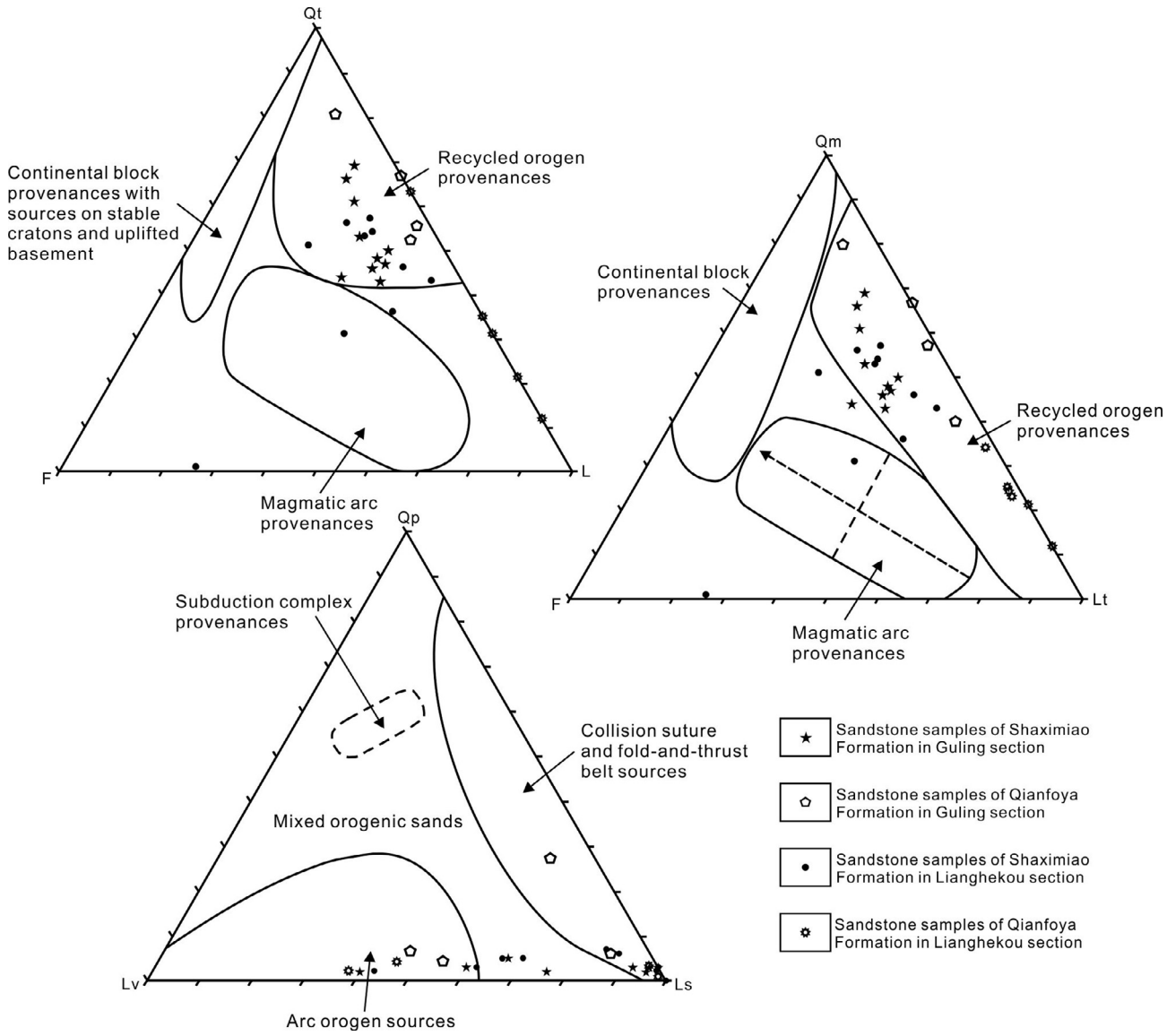

Fig. 4. Ternary plots for Early-Middle Jurassic sandstone composition data from the Lianghekou and Guling sections. Provenance fields are from Dickinson and Suczek (1979). Qt, total quartz; F, plagioclase feldspar and K-feldspar; L, total lithic fragments excluding polycrystalline quartz; Qm, monocrystalline quartz; Lt, total lithic fragments; Qp, polycrystalline quartz (including chert); Lv, volcanic rock fragments; Ls, sedimentary rock fragments (Liu et al., 2005, 2010).

4.2. Lithic composition, petrofacies, and source analyses

The lithic composition data and petrofacies are illustrated in Figs. 3 and 5. The percentage of each petrofacies in Fig. 5 is the normalized percentage of total lithic content in each stratigraphic unit. The petrofacies consists of groups of lithologies that are found together in different source regions, thus defining a distinctive provenance. Lithic petrofacies I consists of abundant chert (Fig. 6a) in the Middle Jurassic strata. There are two potential source areas for the chert fragments. One is the thick chert beds interlayered with limestone of Permian to Early Triassic age exposed in the southern Qinling-Dabieshan fold-thrust belt. The other is the deep-water cherts of the Mianlue oceanic basin (closure of the oceanic basin during the Middle-Late Triassic produced the currently buried part of the Mianlue suture). Although the rocks of the suture zone are no longer exposed, it is possible that deep-water cherts were present. Furthermore, masses of chert pebbles occur at the base of the Lianghekou and Guling sections, which may suggest that seafloor chert of the Mianlue ocean was the source of the chert fragments. If the chert beds interlayered with limestone were the source area, then detrital limestone grains should be common in the sandstone; however, only the Lianghekou section contains significant amounts of limestone (21%). In addition, uplift of Paleozoic rocks by the thrust belt did not take place until the Late Jurassic.

Petrofacies II contains rhyolite (Fig. 6b), trachyandesite, and andesite (Fig. 6c). Andesite accounts for approximately 22% and 10% of the upper Middle Jurassic Shaximiao Formation in the Guling and Lianghekou sections, respectively; however, there is a lack of rhyolite and trachyandesite in this region. The source area for this lithic fragment type was probably the Mianlue suture in western Qinling, where there are limited occurrences of arc-volcanic rocks (Lai and Zhang, 2000) of similar composition, suggesting that the Mianlue suture once extended to the north of the northern Sichuan and Zigui basins, but is now mostly covered by thrust nappes. Upper Triassic strata are widely exposed along the

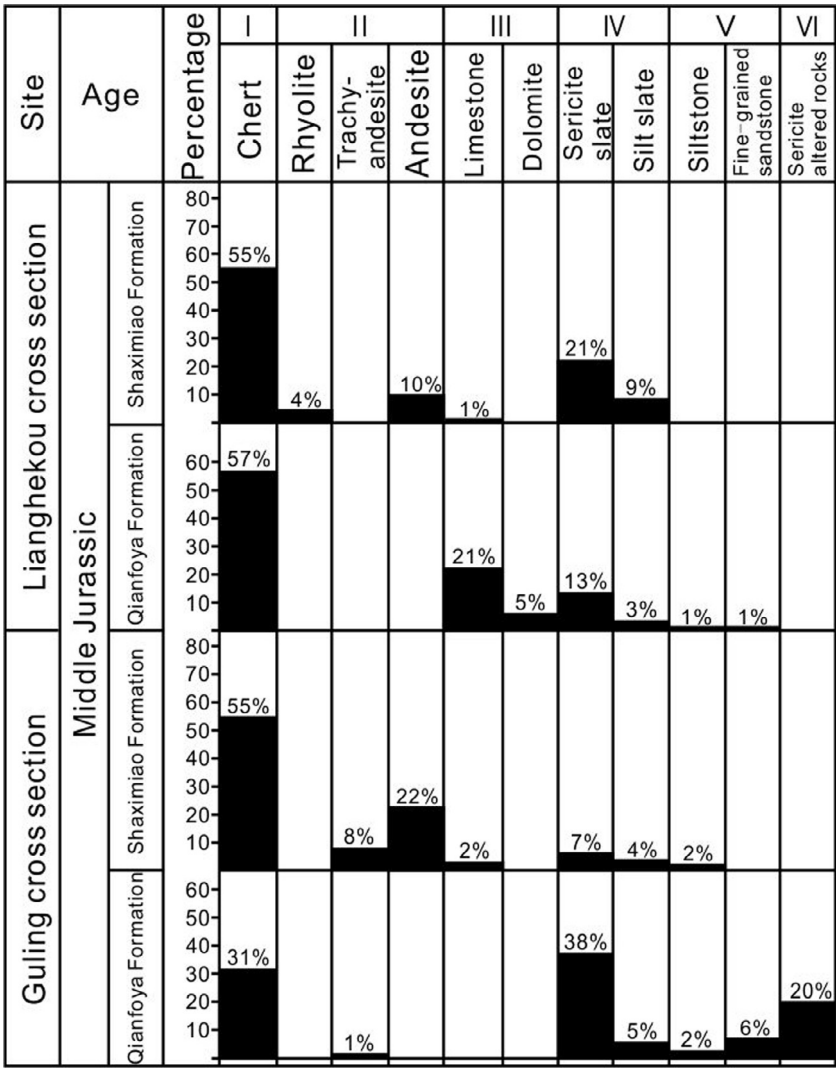

Fig. 5. Summary of lithic petrofacies in the Lianghekou and Guling cross-sections, northern Sichuan Basin (Liu et al., 2003, 2005).

southern Qinling-Dabieshan fold-thrust belt (Dong et al., 2011), and constituted the sedimentary source for the northern Yangtze basin during the Jurassic.

Petrofacies III includes limestone (Fig. 6d) and dolomite fragments that were possibly derived from Paleozoic to Triassic marine sedimentary units in the Mianlue oceanic basin. Petrofacies IV contains low-grade metasedimentary rocks, sericite-bearing slate (Fig. 6e), and silty slate. The source area for Petrofacies IV includes Silurian rocks of the Qinling-Dabieshan orogenic belt (Bureau of Geology and Mineral Resources of Shaanxi, 1991).

Petrofacies IV contains a small number of sedimentary lithic fragments of siltstone and fine-grained sandstone (Fig. 6f). Cessation of marine sedimentation and a progressive change to continental strata took place in the northern Yangtze plate during the Middle and Late Triassic; therefore, Upper Triassic-Lower Jurassic terrigenous clastic sedimentary rocks probably served as the source areas. The scarcity of sericitized rocks (Petrofacies V) (Fig. 6g) indicates that these rocks were barely exposed prior to the Jurassic.

Chert, andesite, limestone, and sericite-bearing slate are the main lithologies in Middle Jurassic rocks. Source areas in the Mianlue suture belt provided some detritus to the Jurassic northern Yangtze foreland basin, particularly chert fragments. The prior to closure of the Mianlue oceanic basin provided limestone fragments from upper Paleozoic shelf deposits. Beginning in the Middle Jurassic, andesite debris was unroofed from a volcanic-arc source area exposed in the Qinling-Dabieshan orogenic belt. Although it is unclear when the volcanic arc was active, the regional tectonic setting indicates that arc formation occurred. Another lithic type, sericite-bearing slate, was probably also derived from the Qinling-Dabieshan belt, especially the Silurian rocks of that area.

5. U-Pb ages and trace elements of detrital zircon

Samples NX and GL are medium- to coarse-grained sandstone from the lower Middle Jurassic Qianfoya Formation from Nanxi and the upper Middle Jurassic Shaximiao Formation from Guling, respectively; both localities are in the northern Sichuan Basin (see Fig. 1 for sample locations). A total of 105 single detrital zircons from NX were dated, yielding 93 usable data, and 132 single detrital zircons from GL were dated, yielding 112 usable data. In addition, we cited data from one sandstone sample from the Qianfoya Formation at the northeastern margin of the Sichuan Basin and two from the Shaximiao Formation along the eastern margin of the Sichuan Basin, from previous studies (Li et al., 2010; Luo et al., 2014; sample locations are marked in Fig. 1).

Cathodoluminescence (CL) images clearly show that most of the analyzed zircons, ranging from 64 to 294 μm in size, display oscil-

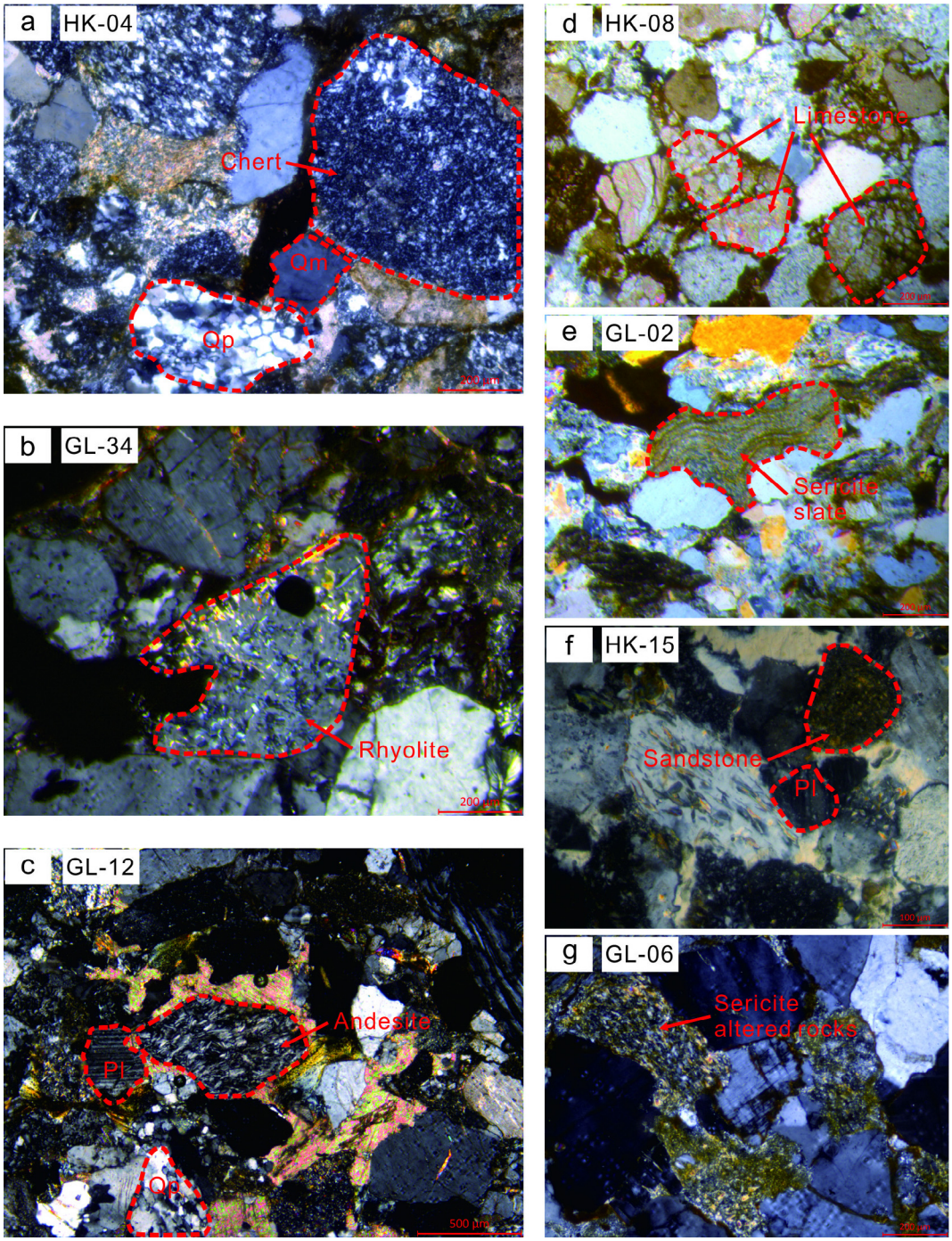

Fig. 6. Photomicrographs under orthogonal light showing lithic composition chert of HK-04(a), rhyolite of GL-34(b), andesite of GL-12(c), limestone of HK-08(d), sericite slate of GL-02(e), sandstone of HK-15(f) and sericite altered rocks of GL-06(g). See locations of thin sections in Fig. 3.

latory zoning and some sector/planar zoned or unzoned complicated internal structures (Fig. 7). Most of the dated zircons are columnar; a few are granular or irregularly shaped. The zircons are sub-rounded to rounded, possibly indicating distal source areas and long-distance transportation. Some angular-subangular zircons with typical igneous oscillatory zoning are probably products of tectonic magmatism. In contrast, zircons with white or gray rims in CL images underwent strong crystallization that resulted in replacement of the primary oscillatory zoning: these crystals yield ages older than 1000 Ma. It is generally possible to estimate zircon genesis on the basis of Th/U ratios: values of more than 0.4 are indicative of a magmatic origin; values less than 0.1 suggest a metamorphic origin (Hoskin, 2002). However, it has been reported that the Th/U ratios of some magmatic origin zircons are less than 0.1 and of some metamorphic ones are more than 0.1 (Pidgeon, 1992; Hidaka et al., 2002). Therefore, comprehensive analysis of internal structures, Th/U ratios, and rare earth elements is necessary to investigate zircon origins.

5.1. Th/U ratios and rare earth elements

The analyzed zircons of the NX sandstone sample exhibit Th/U ratios of 0.19–4.31, of which 78 grains (83%) have ratios higher than 0.4, and no grains exhibit ratios of less than 0.1 (see the

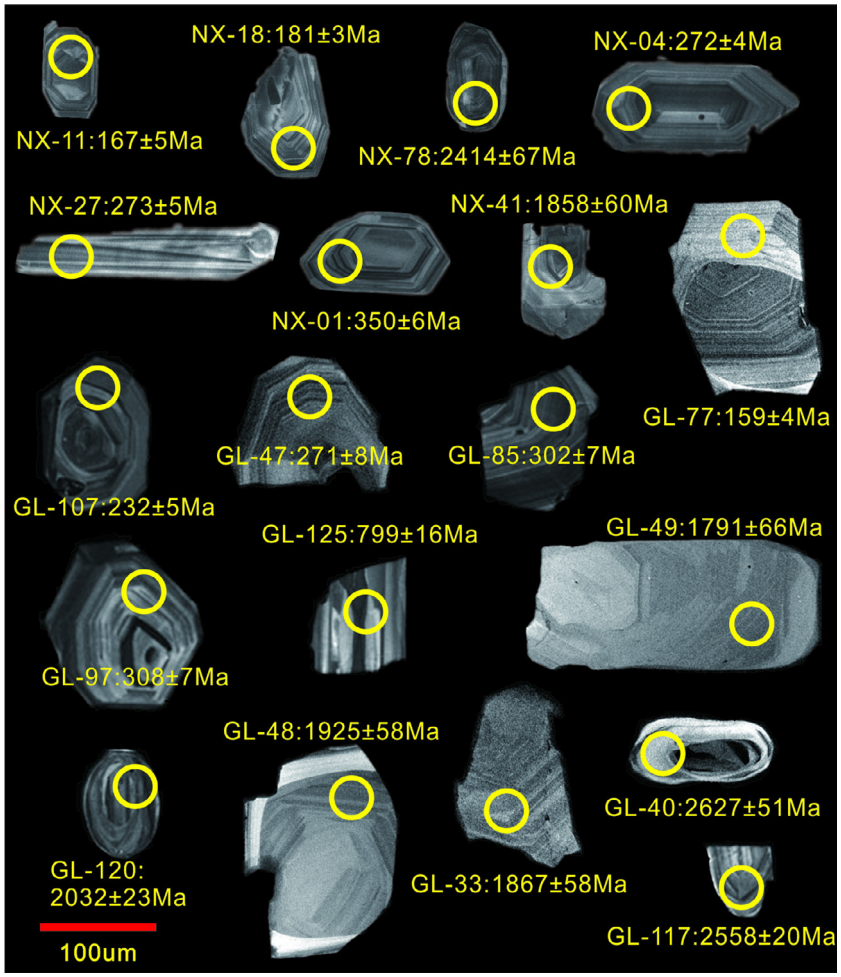

Fig. 7. Representative cathodoluminescence images of zircons.

Supporting Information). Most of the NX sample zircons have variable but generally high chondrite-normalized total rare earth element (REE) concentrations of 213.98–2046.66 ppm and are characterized by distinct enrichment in heavy rare earth elements (HREEs) ($[Lu/Gd]_N$ = 5.04–51.46), depletion in light rare earth elements (LREEs), steep HREE patterns ($[Yb/Sm]_N$ = 3.93–180.22), a large positive Ce anomaly (δCe = 1.11–421.76), and a negative Eu anomaly (δEu = 0.007–1.29; Fig. 8; see also Supporting Information). These values, plus evidence from the CL images, suggest an igneous origin (Vavra et al., 1996; Miller et al., 1998) (Fig. 7). Similarly, the CL images show that typical igneous oscillatory zoning dominates the GL sandstone sample, in which most of the Th/U ratios are greater than 0.4 (approximately 88 grains see Supporting Information). The grains, from this sample also show enrichment of chondrite-normalized REE concentrations, steep HREE patterns ($[Yb/Sm]_N$ = 6.08–295.51), and negative Eu anomalies (δEu = 0.01–0.77; Fig. 8; see also Supporting Information). Otherwise, a few zircons from samples NX and GL that have lower negative Eu anomalies consistently exhibit sector/planar zonation or are not zoned and have shiny-rim internal structures (GL-40 and GL-48 in Fig. 7) that indicate a metamorphic origin for these grains.

5.2. Detrital zircon populations and potential source areas

The analyzed zircon U-Pb ages of Middle Jurassic strata can be correlated with discrete source areas in the Qinling-Dabieshan orogen in the north, the Mianlue suture zone, and the South China plate in the south.

Nearly all the analyzed zircons show less than 10% discordance on concordia plots (Fig. 9). For the NX sandstone, U-Pb dating yielded four major zircon populations: 167–197 Ma (peak age 176 Ma); 207–299 Ma (peak age 265 Ma); 313–476 Ma (peak age 370 Ma); and 1650–2487 Ma (peak ages 1880 and 2480 Ma). For the GL sandstone, U-Pb dating yielded six major zircon age populations: 158–188 Ma (peak age 160 Ma); 220–292 Ma (peak ages 221 and 274 Ma); 302–369 Ma (peak age 368 Ma); 711–831 Ma (peak age 812 Ma); 1572–2494 Ma (peak ages 1888 and 2488 Ma); and 2512–2777 Ma (Fig. 10).

According to the youngest concordant age obtained from the sample, which is identical to the maximum depositional age of the sedimentary rocks (Greentree et al., 2006; Wang et al., 2012), the timing of deposition of the Qianfoya and Shaximiao formations were later than 167 ± 5 Ma and 158 ± 7 Ma, respectively.

5.2.1. Detrital zircons with ages of 167–197 and 158–188 Ma

The zircon populations with ages of 167–197 and 158–188 Ma comprise 19 grains (20%) from the Qianfoya Formation and 12 grains (12%) from the Shaximiao Formation, respectively. The CL and trace-element data (Th/U ratios exceed 0.4 for 85% of grains; see the Supporting Information) indicate that most of the population is of magmatic origin and that the peaks at ~176 Ma and ~160 Ma in the zircon populations are probably consistent with the ages of the magmatic rocks of the northern Yangtze foreland

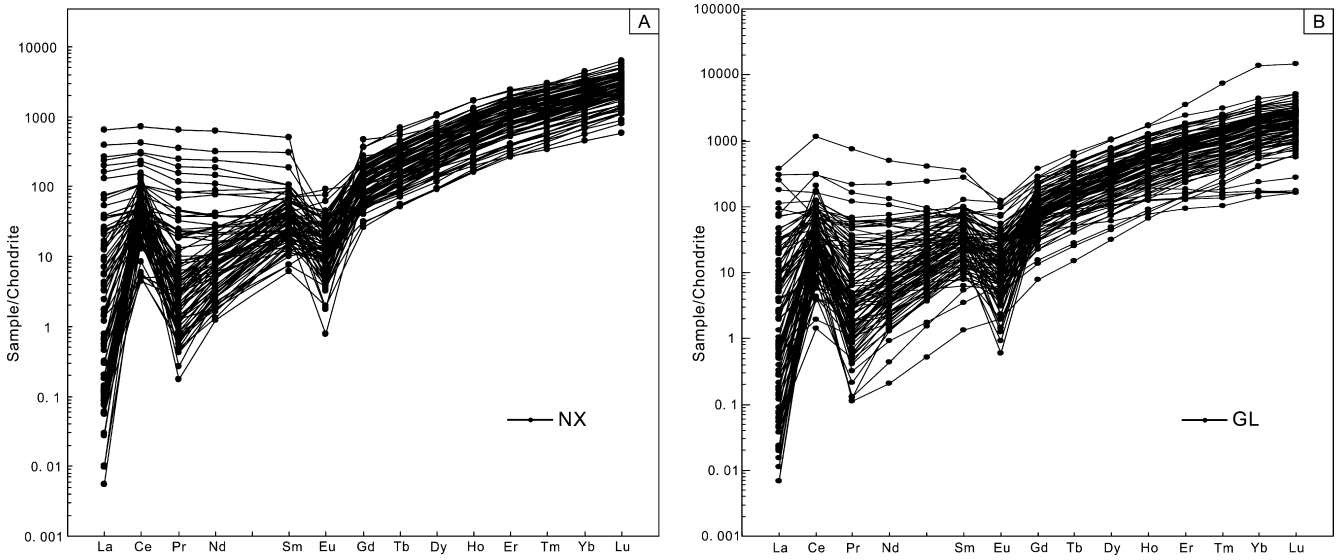

Fig. 8. Chondrite-normalized REE patterns for zircons from the (A) NX and (B) GL sandstone samples from the Nanxi and Guling sections, respectively. Chondrite REE values are from Sun and McDonough (1989).

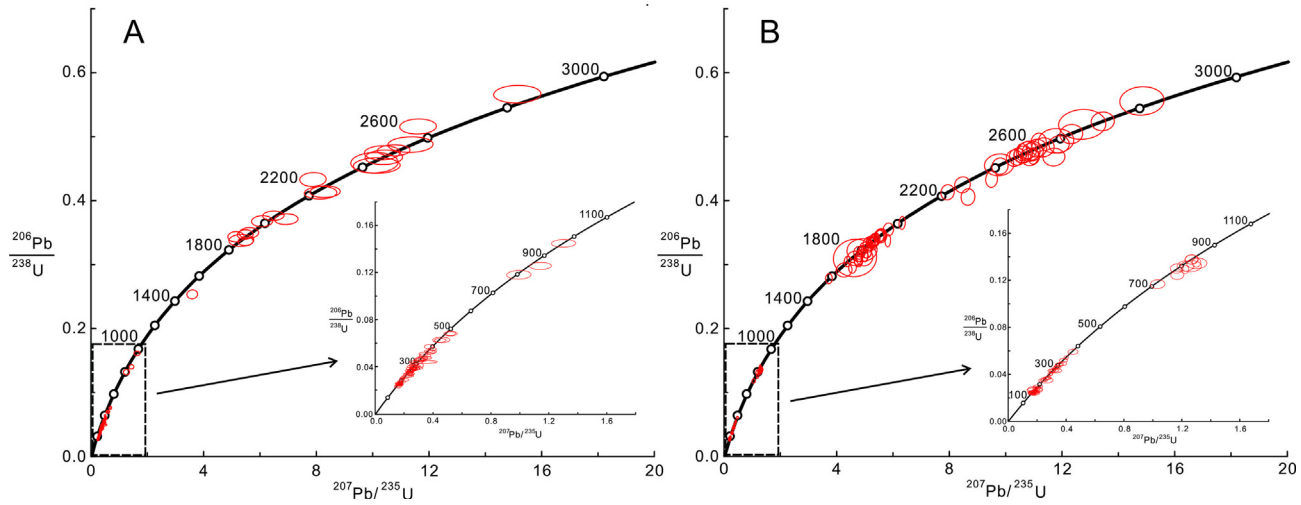

Fig. 9. Concordia plots of zircons from medium- to coarse-grained sandstones from the Nanxi (A) and Guling (B) sections.

basin. Although Yanshanian magmatism is evidenced by the granitic rocks in north Qinling (Zhang et al., 2001; Dong et al., 2011) (Fig. 11), during the Middle-Late Triassic the Yangtze plate obliquely collided with the North China-Qinling-Dabieshan plates and collision progressed from east to west. Subsequently, the molasse foreland basin of the northern margin of the Yangtze plate experienced compression tectonism, which resulted in magmatism during the Late Triassic and Early Jurassic. However, the burial or covering up of these magmatic rocks resulted from later thrusting related to the fold-thrust belt of the southern Qinling-Dabieshan orogeny.

5.2.2. Detrital zircons with ages of 207–299 Ma and 220–292 Ma

A relatively large number of Permian-Triassic detrital zircons were found in the NX and GL samples, accounting for 35% and 14% of the total number of zircons in each sample, respectively. Higher Th/U ratios (only one grain with a value of <0.4), trace-element data, and clear oscillatory zoning suggest a magmatic origin. The age peak at ~221 Ma in the Permian-Triassic zircon population is consistent with Triassic continental collision and subduction in the Qinling-Dabieshan orogen along the Mianlue suture zone; this period age is particularly widely distributed in south Qinling (Figs. 11 and 12). Although the peaks at ~265 and ~274 Ma are rarely found in the Qinling orogenic belt, this zircon population can be interpreted as an influx of material derived from erosion of the Mianlue suture zone, as evidenced by seismic structures that formed in the region of the Qinling-Dabieshan orogen during the Late Paleozoic to Early Triassic, but that are now largely buried by later long-distance overthrusting (Zhang et al., 2001; Liu et al., 2015a, 2015b). Therefore, the south Qinling and Mianlue suture zones are potential source areas for these zircon populations.

5.2.3. Detrital zircons with ages of 313–476 and 302–369 Ma

This population with ages of 313–476 and 302–369 Ma comprise 35% from the NX and 0.05% from the GL sandstone sample, respectively. The Paleozoic detrital zircon signature corresponds to the distribution of Paleozoic volcanic rocks and granitoids along the southern Qinling-Dabieshan orogen (Fig. 11), which potentially were exhumed by thrusting. The peak ages of ~370 and ~368 Ma

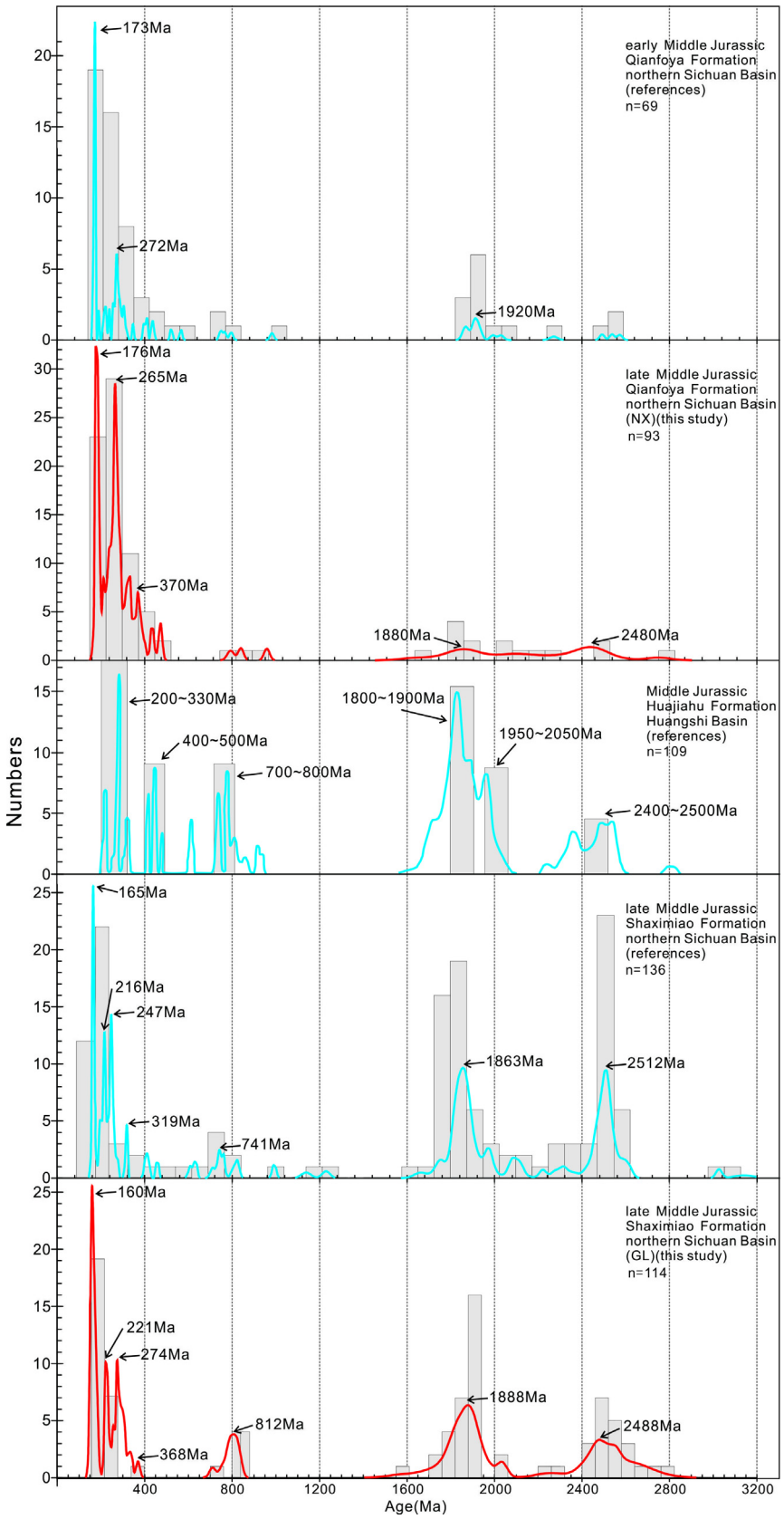

Fig. 10. Probability density populations showing the LA-ICP-MS dating of detrital zircons from the lower Middle Jurassic Qianfoya Formation of the Nanxi section (NX) and the upper Middle Jurassic Shaximiao Formation of the Guling section (GL). The locations of sampling sites are marked in Fig. 1. Data from previous studies are from She (2008), Li et al. (2010), Yang et al. (2010), and Luo et al. (2014).

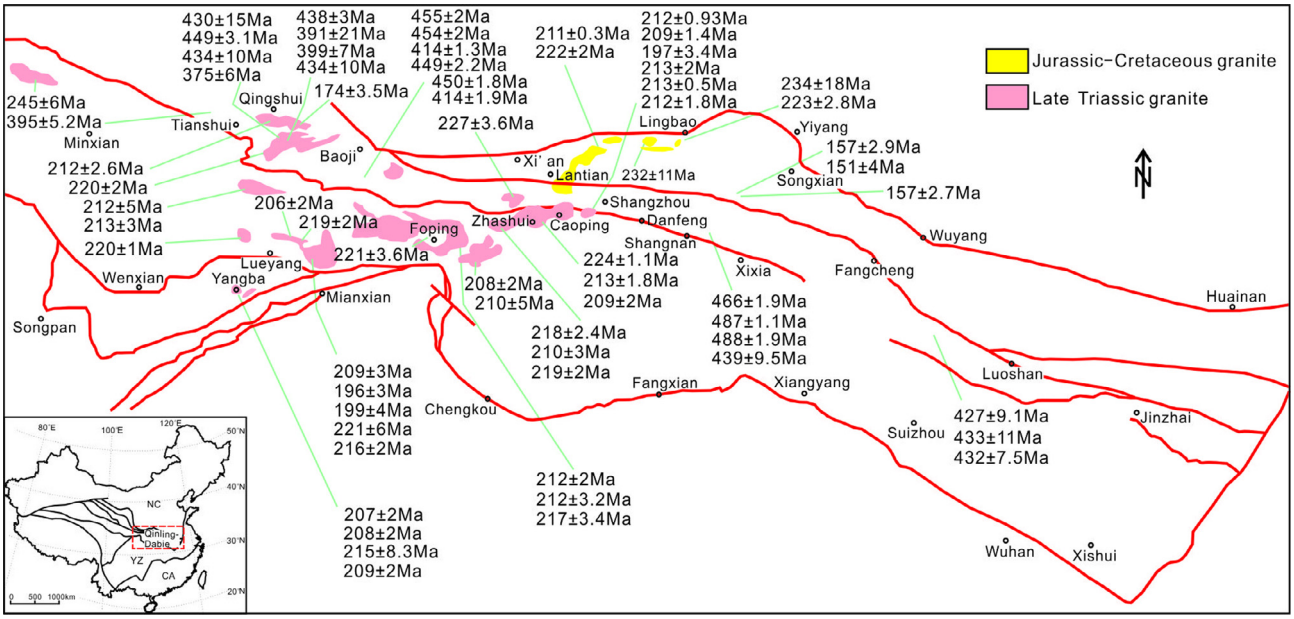

Fig. 11. Distribution of Late Triassic-Cretaceous granites and their ages in the Qinling-Dabie orogenic belt (modified from Dong et al. (2011)).

are consistent with the age of closure of the Shangdan oceanic basin and north-directed subduction of south Qinling underneath north Qinling (Zhang et al., 2001; Dong et al., 2011).

5.2.4. Detrital zircons with ages of 800–967 and 711–831 Ma

The Neoproterozoic detrital zircon population displays age peaks at ~856 and ~812 Ma for the NX and GL samples, respectively (Fig. 10). All the Th/U ratios of zircon grains exceed 0.4 and CL images are characterized by clear oscillatory zoning, suggesting a magmatic origin. Abundant data from the literature indicate that these age populations are widely distributed in north Qinling (peak age ~744 Ma), south Qinling (peak age ~751 Ma), the Yangtze plate (peak age ~788 Ma), and the South China plate (peak age ~835 Ma; Fig. 12). The age data probably suggest that this zircon population was derived from those areas. Neoproterozoic rift-related magmatism in the Qinling and northern Yangtze areas has been documented by Zhou et al. (1998; 743 ± 12 Ma), Ling et al. (2001; 785 ± 88 Ma), Lu et al. (2005; 711 ± 11, 723 ± 3, 731 ± 1, and 808 ± 6 Ma), and Li et al. (2003; 808 ± 6 Ma). Collision between the Yangtze and North China-Qinling-Dabie plates during the Jurassic resulted in uplift and erosion of older rocks, which provided detrital sediments to the northern Yangtze foreland basin.

5.2.5. Detrital zircons with ages of 1650–2487 and 1706–2494 Ma

The detrital zircon population with Late Paleoproterozoic ages (peak ages of ~1880, ~2480, and ~2488 Ma) is abundant in the NX and GL sandstone samples, accounting for 19% and 43% of total zircon grains, respectively. Of this Late Paleoproterozic population, 32% of zircon grains show Th/U ratios of less than 0.4, together with shiny rims in CL images (Fig. 7), possibly indicating a metamorphic origin. These age ranges are correlated with a well-documented series of thermal events that occurred between 1.9 and 1.8 Ga on the South China plate, which is also consistent with the U-Pb age patterns of detrital zircons from the basement rocks of the northern Yangtze plate and southern North China plate (Fig. 12). However, the Yangtze plate was subducted northward beneath the Qinling-Dabieshan microplate at the same time as north Qinling was thrust northward onto the North China plate during the Late Triassic; consequently, the detrital sediments of the southern North China plate could not reach the Yangtze foreland basin. The ages of these zircons indicate their derivation from basement rocks or from recycled materials on the south China plate. The predominant westward and northwestward paleocurrents are consistent with a provenance from the east or southeast. The source of this zircon group was probably the northern South China plate (the northern Yangtze plate).

5.2.6. Detrital zircons with ages of 2512–2777 Ma

A small number of zircon grains yield ages of 2512–2777 Ma. Some of the zircon grains have an igneous origin, and the other a metamorphic origin. The Neoarchean zircon and Paleoproterozoic zircon populations correspond with magmatic events identified in the Kongling Complex and Huangtuling granulites from the Yangtze plate (Zhang et al., 2006; Liu et al., 2008). The source of this zircon group was likely located south or southeast of the northern Yangtze foreland basin. Intensive thrusting in the Qinling-Dabieshan orogen led to the exhumation of basement rocks or the recycling of material from the South China plate (Fig. 12).

6. Discussion

The unroofing history recorded by sandstone composition in the basin sedimentary sequence provides a useful indicator of the uplift and erosional evolution of the adjacent orogenic belt (Hendrix et al., 1996; Hendrix, 2000). Thus, the lithic composition, petrofacies, ternary plots of sandstone composition data, paleoflow directions, and detrital zircon LA-ICP-MS age data can provide insights into the sediment provenance of the northern Yangtze foreland basin, its significance for the syndepositional basin-mountain pattern, and certain geological units that existed in the past but are no longer visible through being modified or covered by later thrusting and shortening orogenesis following the oblique collision between the North China-Qinling-Dabieshan and Yangtze complex plates. During deposition of the Baitianba Formation, the continental molasse foreland basin started to form. During deposition of the Qianfoya Formation, meandering river and lake deposits accumulated. The thicknesses of the Baitianba and Qianfoya formations indicate that the thrust belts of the peripheral basin did not create a large tectonic load that contributed to subsidence. An

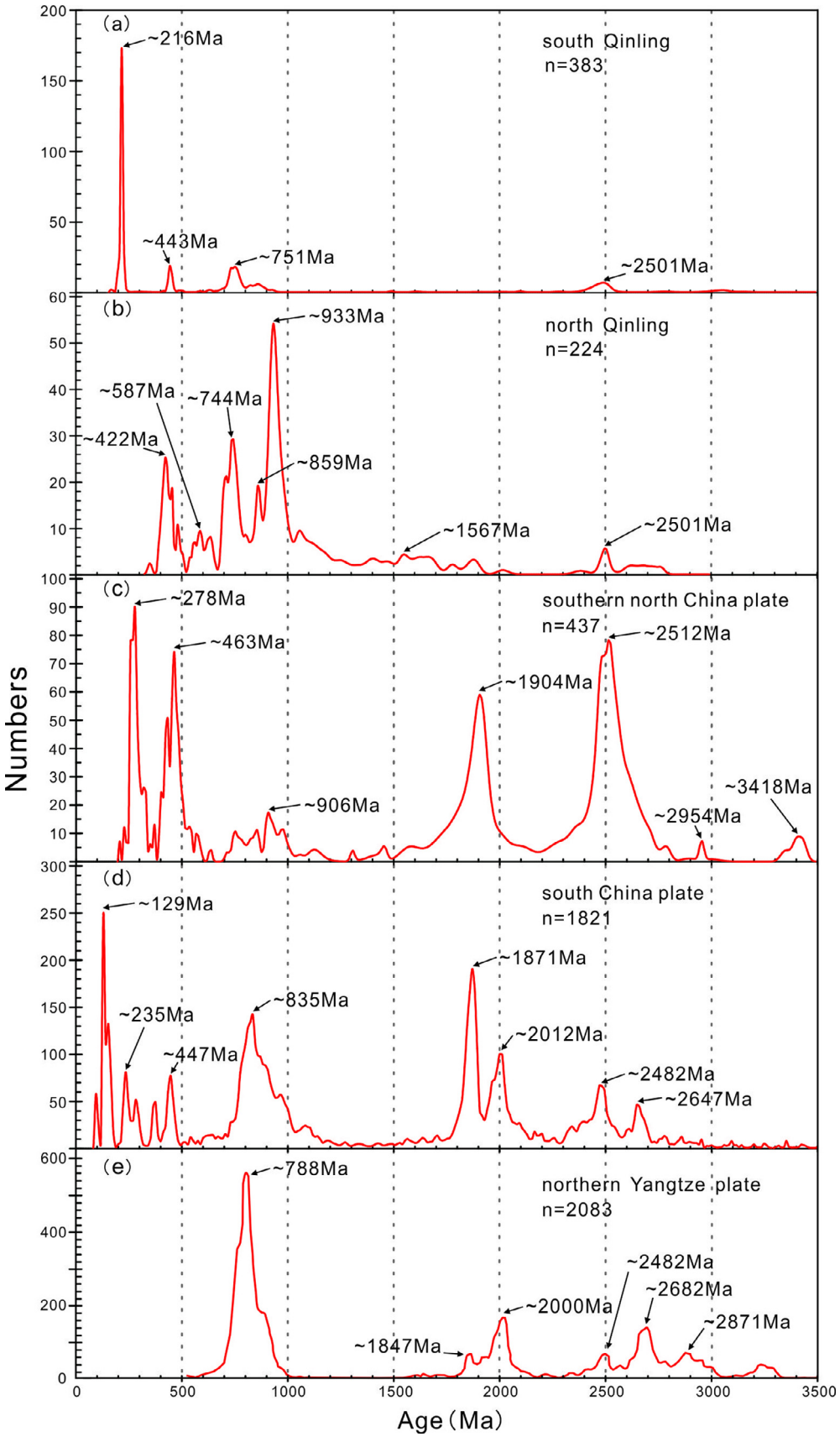

Fig. 12. Probability density populations of detrital zircons of the Qinling-Dabieshan orogen, southern North China plate, South China plate, and northern Yangtze plate. Age data are from (a) south Qinling (Zhu et al., 2011; Ping et al., 2013; Qin et al., 2013; Shi et al., 2013); (b) north Qinling (Shi et al., 2009, 2013); (c) the southern North China plate (Wan et al., 2006; Cui et al., 2011; Shi et al., 2011; Diwu et al., 2012); (d) the South China plate (Xu et al., 2007; Liu et al., 2008; Li et al., 2012; Peng et al., 2012; Wang et al., 2014); and (e) the northern Yangtze plate (Luo et al., 2014).

insufficient sediment supply resulted in thick-bedded siltstone and mudstone units. The Shaximiao Formation contains thickly bedded, braided-river delta successions with a maximum thickness of 2000 m. Strong tectonic activity in the orogenic belts contributed to flexural subsidence and provided sufficient accommodation space for the deposition of sediments. Furthermore, the orogen experienced exhumation and provided abundant sediments to the foreland basin. The Shaximiao Formation was probably deposited during the main period of basin formation and was a response to intense thrusting in the adjacent orogenic belts.

Medium- to coarse-grained sandstone with well-developed tabular, wedge, and trough cross- bedding, which formed in the Lower-Middle Jurassic thickly bedded river-belt, occurs widely in the northern Yangtze foreland basin. The paleoflow directions in the Wangcang area (located to the south of Micangshan fold-thrust belt) and the Huangzhong area (in front of Dabashan fold-thrust belt) were mostly north-south (Fig. 13), suggesting that the basin sediments were derived from the Qinling-Dabieshan orogen and/or the Mianlue suture belt. Paleocurrent indicators in the Lianghekou area, located at the intersection of the Micangshan and Dabashan, in the Guling and Jiagao sections, and in the Xietan and Xiakou areas of the Zigui Basin are east-west, southeast-northwest, and locally southwest-northeast (Fig. 13), indicating that sediment in the northern Yangtze foreland basin was supplied from geological bodies to the west and/or south. The occurrence of two paleoflow directions, south-directed transverse flow that was nearly perpendicular to the northern fold-thrust belt and west-directed longitudinal flow that was parallel to the direction of basin extension, is characteristic features of the foreland basin. The northern foreland fold-thrust belt and backbulge depozone of the Yangtze foreland basin are potential source areas that provided sedimentary detritus during the Early-Middle Jurassic.

The multiple zircon age populations and the various paleocurrent data indicate sediment influx from the north, northeast, east, and southeast. This observation implies that materials were derived from the Qinling-Dabieshan orogen and the Mianlue suture zone, both of which are consistent with the south- or southeast-directed paleoflow, and the South China plate, consistent with the west- or northwest-directed paleoflow. Chert and limestone were derived largely from the currently buried Mianlue suture, which is referred to as the "collision suture" in the ternary diagrams. Andesite, granitoid, and sericite-bearing slate were probably derived from a recycled orogen or fold-thrust belt, particularly the Qinling-Dabieshan orogenic belt. Samples from the lower Middle Jurassic Qianfoya Formation contain major Jurassic, Permian-Triassic, Paleozoic, and Late Paleoproterozoic zircon populations, indicating the Qinling-Dabieshan orogen, Mianlue suture zone, and South China plate as sources. The samples from the upper Middle Jurassic Shaoximiao Formation exhibit the same characteristics as those from the Qianfoya Formation, except for the occurrence of Neoproterozoic and Neoarchean age groups and an increase in the influx of Late Paleoproterozoic zircons. This observation suggests that increased infilling and longitudinal bypassing of sediments derived from the South China plate occurred during the Middle Jurassic. Therefore, the Middle Jurassic northern Yangtze foreland basin was fed longitudinally along the basin from the eastern source areas; i.e., from the Qinling-Dabieshan orogen and collisional Mianlue suture to the north, and from the South China plate to the south.

The think stratigraphic succession of late Middle Jurassic age may be related to its longer duration of sedimentation; similarly, the increase in the influx of Neoproterozoic, Late Paleoproterozoic, and Neoarchean zircons suggests that more intense thrusting resulted in the exhumation and erosion of basement rocks. These inferences all indicate that contractional tectonism during the Early-Middle Jurassic followed the Middle-Late Triassic collision-induced orogenesis, which resulted in frequent magmatic activity in the source areas, denudation of the sedimentary cover in south Qinling, and modification or burial of the Mianlue suture zone, island-arc units, and nonmarine molasse foreland basin of the northern Yangtze plate during the Middle-Late Triassic.

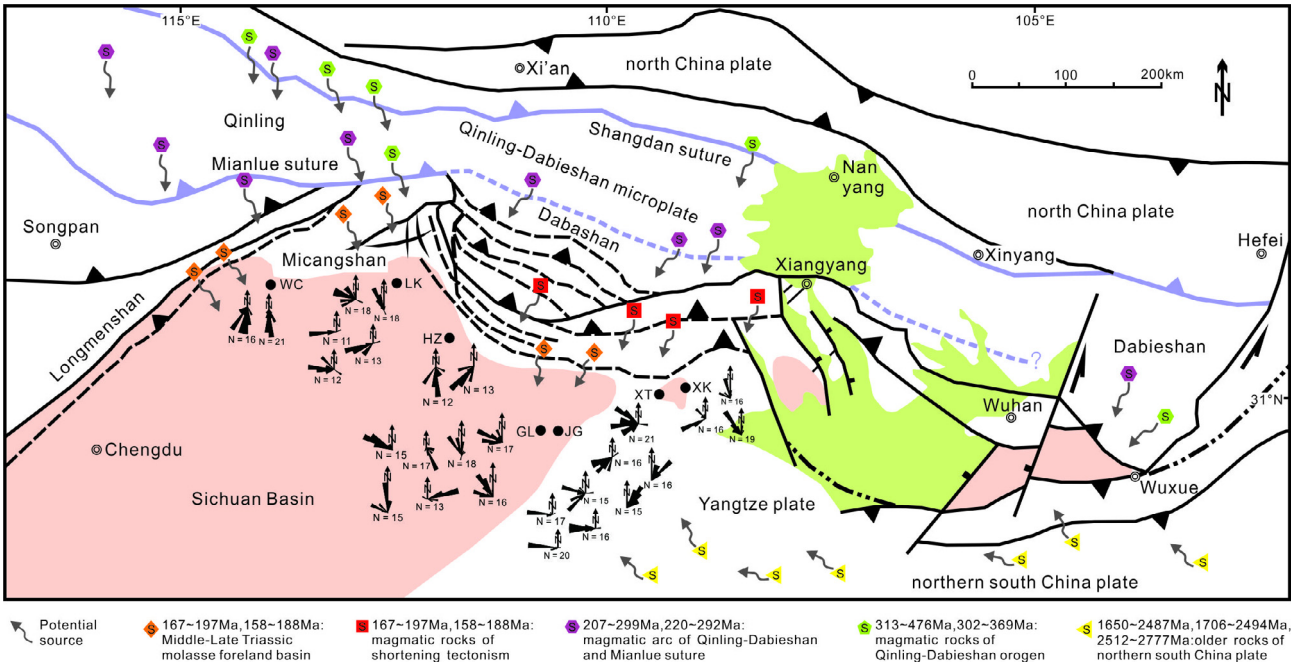

Fig. 13. Paleocurrent directions and interpreted provenance plotted on the tectonic framework of the study area. Gray arrows indicate generalized sediment dispersal directions. Paleocurrent directions were measured from well-developed tabular, wedge, and trough cross-stratifications of Lower-Middle Jurassic sandstone bodies, northern middle-upper Yangtze foreland basin. WC, Wangcang; LK, Lianghekou; HZ, Huangzhong; GL, Guling; JG, Jiagao; XT, Xietan; XK, Xiakou. The other symbols are the same as in Fig. 1.

7. Conclusions

(1) During deposition of the Shaximiao Formation, which consists of thick-bedded deposits, intense tectonic activity in the southern Qinling-Dabieshan fold-thrust belt resulted in loading-related subsidence that contributed to the formation of the foreland basin.
(2) Lithic composition and petrofacies data suggest that the basin sediments were derived from collision suture, fold-thrust belt, and recycled orogen. Middle Jurassic sandstone samples from the northern Yangtze foreland basin yield zircon age populations of Jurassic, Permian-Triassic, Paleozoic, Neoproterozoic, Late Paleoproterozoic, and Neoarchean. The source areas that fed into the basin were the Mianlue suture zone, the Qinling-Dabieshan orogenic belt, and the South China plate. These source areas are consistent with the two main paleocurrent directions: south- and southeast-directed lateral paleoflow, and west- and northwest-directed longitudinal paleoflow.
(3) The Mianlue oceanic basin, magmatic arc, and nonmarine molasse foreland basin that developed early during the period of deposition were modified or buried by Jurassic compression between the North China-Qinling-Dabieshan plate and Yangtze plate, which followed the oblique amalgamation between these plates during the Middle-Late Triassic.

Acknowledgements

We thank the Editor-in-chief Dr. Meifu Zhou and Miss Diane Chung, and two anonymous reviewers for their critical, helpful, and insightful comments. The authors also deeply thank Andong Zhang, Chao Li, and Huili Ji for their LA-ICP-MS experiment assistance. Financial support was provided by the National Natural Science Foundation of China (grant numbers 41030318 and 91114203); and Specialized Research Fund for the Doctoral Program of Higher Education of China (grant number 20130022110002).

Appendix A. Supplementary material

Supplementary data associated with this article can be found, in the online version, at http://dx.doi.org/10.1016/j.jseaes.2016.09.016.

References

Allen, J.R.L., 1978. Studies in fluviatile sedimentation: an exploratory quantitative model for the architecture of avulsion-contronlled alluvial suites. Sed. Geol. 21, 129–147.
Bureau of Geology and Mineral Resources of Shaanxi, 1991. Regional Geology of Sichuan Province. Geological Publishing House, Beijing, pp. 1–698.
Cui, M.L., Zhang, B.L., Zhang, L.C., 2011. U-Pb dating of baddeleyite and zircon from the Shizhaigou diorite in the southern margin of North China Craton: constrains on the timing and tectonic setting of the Paleoproterozoic Xiong'er group. Gondwana Res. 20, 184–193.
Dickinson, W.R., Suczek, C.A., 1979. Plate tecttonics and sandstone compositions. Am. Assoc. Petrol. Geol. Bull. 63, 2164–2182.
Diwu, C.R., Sun, Y., Zhang, H., Wang, Q., Fan, L.G., 2012. Episodic tectonothermal events of the western North China Craton and North Qinling Orogenic Belt in central China: Constraints from detrital zircon U-Pb ages. J. Asian Earth Sci. 47, 107–122.
Dong, Y.P., Zhang, G.W., Neubauer, F., Liu, X.M., Genser, J., Hauzenberger, C., 2011. Tectonic evolution of the Qinling orogen, China: review and synthesis. J. Asian Earth Sci. 41, 213–237.
Enkin, R., Yang, Z., Chen, Y., Courtillot, V., 1992. Paleomagnetic constraints on the geodynamic history of China from Permian to present. J. Geophys. Res. 97, 13953–13989.
Gilder, S.A., Courtillot, V., 1997. Timing of the north-south China collision from new middle to late Mesozoic paleomagnetix data from the North China block. J. Geophys. Res. 120, 17713–17727.
Greentree, M.R., Li, X.H., Wu, H.C., 2006. Late Mesoproterozoic to earliest Neoproterozoic basin record of the Sibao orogenesis in western South China and relationship to the assembly of Rodinia. Precambrian Res. 15, 79–100.
Hendrix, M.S., Graham, S.A., Amory, J.Y., Badarch, G., 1996. Noyon Uul (King Mountain) syncline southern Mongolia: lower Mesozoic sedimentary record of the tectonic amalgamation of central Asia. Geol. Soc. Am. Bull. 108, 1256–1274.
Hendrix, M.S., 2000. Evolution of Mesozoic sandstone compositions, southern Junggar, northern Tarim, and western Turpan basins, northwest China: a detrital record of the ancestral Tian Shan. J. Sed. Res. 70, 520–532.
Hidaka, H., Shimizu, H., Adachi, M., 2002. U-Pb geochronology and REE geochemistry of zircons from Palaeoproterozoic paragneiss clasts in the Mesozoic Kamiaso conglomerate, central Japan: evidence for an Archean provenance. Chem. Geol. 187, 278–293.
Hoskin, P.W.O., 2002. Rare earth element chemistry of zircon and its use as a provenance indicator. Geology 28, 627–630.
Lai, S.C., Zhang, G.W., 2000. Idntification of the island-arc magmatism zone in the Lianghe-Raofeng-Wuliba area, south Qinling and its tectonic significance. Sci. China (Ser. D): Earth Sci. 43, 69–81 (in Chinese with English abstract).
Li, H.K., Lu, S.N., Chen, Z.H., Xiang, Z.Q., Zhou, H.Y., Hao, G.J., 2003. Zircon U-Pb geochronology of rift-type volcanic rocks of the Yaolinghe Group in the South Qinling orogen. Geol. Bull. China 22, 776–781 (in Chinese with English abstract).
Li, R.B., Pei, X.Z., Liu, Z.Q., Li, Z.C., Ding, S.P., Liu, Z.G., Zhang, X.F., Chen, G.C., Chen, Y. X., Wang, X.L., 2010. Basin-Mountain coupling relationship of foreland basin between Dabashan and northeastern Sichuan—the evidence from LA-ICP-MS U-Pb dating of the detrital zircons. Acta Geol. Sinica 84, 1118–1134 (in Chinese with English abstract).
Li, W.P., Liu, S.F., Qian, T., Dou, G.X., Gao, T.J., 2014. Analysis of structural deformation in the North Dabashan thrust belt, South Qinling, central China. Int. Geol. Rev. 56, 1276–1294.
Li, Z.W., Liu, S.G., Chen, H.D., Deng, B., Hou, M.C., Wu, W.H., Cao, J.X., 2012. Spatial variation in Meso-Cenozoic exhumation history of the Longmen Shan thrust belt (eastern Tibetan Plateau) and the adjacent western Sichuan basin: constrains from fission track thermochronology. J. Asian Earth Sci. 47, 185–203.
Ling, W.L., Wang, X.H., Cheng, J.P., 2001. Geochemical features and its tectonic implication of the Jinniangian Wangjiangshan gabbros in the North margin of Yangtze block. Bull. Mineral., Petrol., Geochem. 20, 218–221 (in Chinese with English abstract).
Liu, S.F., Heller, P.L., Zhang, G.W., 2003. Mesozoic basin development and tectonic evolution of the Dabieshan orogenic belt, central China. Tectonics 22, 1038.
Liu, S.F., Li, W.P., Wang, K., Qian, T., Jiang, C.X., 2015a. Late Mesozoic development of the southern Qinling-Dabieshan foreland fold-thrust belt, Central China, and its role in continent-continent collision. Tectonophysics 644–645, 220–234.
Liu, S.F., Qian, T., Li, W.P., Dou, G.X., Wu, P., 2015b. Oblique closure of the northeastern Paleo-Tethys in central China. Tectonics 34, 1–22.
Liu, S.F., Steel, R., Zhang, G.W., 2005. Mesozoic sedimentary basin development and tectonic implication, northern Yangtze Block, eastern China: record of continent-continent collision. J. Asian Earth Sci. 25, 9–27.
Liu, S.F., Zhang, G.W., Ritts, B.D., Zhang, H.P., Gao, M.X., Qian, C.C., 2010. Tracing exhumation of the Dabie Shan ultrahigh-pressure metamorphic complex using the sedimentary record in the Hefei Basin, China. Geol. Soc. Am. Bull. 122, 198–218.
Liu, X.M., Gao, S., Diwu, C.R., Ling, W.L., 2008. Precambrian crustal growth of Yangtze Craton as revealed by detrital zircon studies. Am. J. Sci. 308, 421–468.
Lu, S.N., Chen, Z.H., Li, H.K., Hao, G.J., Xiang, Z.Q., 2005. Two magmatic belts of the Neoproterozoic in the Qinling orogenic belt. Acta Geol. Sinica 79, 165–173 (in Chinese with English abstract).
Ludwig, K.R., 2003. Mathematical-Statistical treatment of data and errors for ^{230}Th/U geochronology. Rev. Mineral. Geochem. 52, 631–656.
Luo, L., Qi, J.F., Zhang, M.Z., Wang, K., Han, Y.Z., 2014. Detrital zircon U-Pb ages of Late Triassic-Late Jurassic deposits in the western and northern Sichuan Basin margin: constraints on the foreland basin provenance and tectonic implications. Int. J. Earth Sci. 103, 1553–1568.
Miller, C.F., Hatcher, R.D., Harrison, T.M., Gorisch, E.B., 1998. Crytic crustal events elucidated through zone imaging and ion microprobe studies of zircon, southern Appalachian Blue Ridge, North Carolina Georgia. Geology 26, 419–422.
Nie, S.Y., Yin, A., Rowley, D.B., Jin, Y.G., 1994. Exuhumation of the Dabie Shan ultra-high-pressure rocks and accumulation of the Songpan Ganze flysch sequence, central China. Geology 22, 999–1002.
Peng, M., Wu, Y.B., Gao, S., Zhang, H.F., Wang, J., Liu, X.C., Gong, H.J., Zhou, L., Hu, Z.C., Yuan, H.L., 2012. Geochemistry, Zircon U-Pb age and Hf isotope compositions of Paleoproterozoic aluminous A-type granites from the Kongling terrain, Yangtze Block: constraints on petrogenesis and geologic implications. Gondwana Res. 22, 140–151.
Pidgeon, R.T., 1992. Recrystallisation of oscillatory zoned zircon: Some geochronological and petrological implications. Contribut. Minaral. Petrol. 110, 463–472.
Ping, X.Q., Zheng, J.P., Zhao, J.H., Tang, H.Y., Griffin, W.L., 2013. Heterogeneous sources of the Triassic granitoid plutons in the southern Qinling orogen: an E-W tectonic division in central China. Tectonics 32, 396–416.
Qin, J.F., Lai, S.C., Li, Y.F., 2013. Multi-stage granitic magmatism during exhumation of subducted continental lithosphere: evidence from the Wulong pluton, South Qinling. Gondwana Res. 24, 1108–1126.
She, Z.B., 2008. Detrital Zircon Geochronology of the Upper Proterozoic-Mesozoic clastic rocks in the Mid-Upper Yangtze region Ph.D. thesis. China University of Geosciences, Wuhan, China.

Shi, Y., Yu, J.H., Xu, X.S., Qin, J.S., Chen, L.H., 2009. Geochronology and geochemistry of the Qinling Group in the eastern Qinling Orogen. Acta Petrol. Sinica 25, 2651–2670 (in Chinese with English abstract).
Shi, Y., Yu, J.H., Xu, X.S., Tang, H.F., Qiu, J.S., Chen, L.H., 2011. U-Pb ages and Hf isotope compositions of zircons of Taihua Group in Xiaoqinling area, Shaanxi Province. Acta Petrol. Sinica 27, 3095–3108 (in Chinese with English abstract).
Shi, Y., Yu, J.H., Santosh, M., 2013. Tectonic evolution of the Qinling orogenic belt, Central China: new evidence from geochemical, zircon U-Pb geochronology and Hf isotopes. Precambrian Res. 231, 19–60.
Sun, S.S., McDonough, W.F., 1989. Chemical and isotopic systematics of oceanic basalts: implications for mantle composition and processes. Geol. Soc. Lond., Spec. Publ. 42, 313–345.
Tian, Y.T., Kohn, B.P., Zhu, C.Q., Xu, M., Hu, S.B., 2012. Postorogenic evolution of the Mesozoic Micang Shan foreland basin system, central China. Basin Res. 24, 70–90.
Vavra, G., Gebauer, D., Schmid, R., 1996. Multiple zircon growth and recrystallization during polyphase Late Carboniferous to Triassic metamorphism in granulites of the Ivrea Zone (Southern Alps): an ion microprobe (SHRIMP) study. Contrib. Miner. Petrol. 122, 337–358.
Wan, Y., Wilde, S.A., Liu, D.Y., Yang, C.X., Song, B., Yin, X.Y., 2006. Further evidence for 1.85Ga metamorphism in the Central Zone of the North China Craton: SHRIMP U-Pb dating of zircon from metamorphic rocks in the Lushan area, Henan Province. Gondwana Res. 9, 189–197.
Wang, L.J., Yu, J.H., Griffin, W.L., O'Reilly, S.Y., 2012. Early crustal evolution in the western Yangtze Block: evidence from U-Pb and Lu-Hf isotope on detrial zircons from sedimentary rocks. Precambrian Res. 222–223, 368–385.
Wang, Y.J., Zhang, Y.Z., Fan, W.M., Geng, H.Y., Zou, H.P., Bi, X.W., 2014. Early Neoproterozoic accretionary assemblage in the Cathaysia Block: geochronological, Lu-Hf isotopic and geochemical evidence from granitoid gneisses. Precambrian Res. 249, 144–161.
Xu, X.S., O'Reilly, S.Y., Griffin, W.L., Wang, X.L., Pearson, N.J., He, Z.Y., 2007. The crust of Cathaysia: age, assembly and reworking of two terranes. Precambrian Res. 158, 51–78.
Yan, D.P., Zhou, M.F., Li, S.B., Wei, G.Q., 2011. Structural and geochronological constraints on the Mesozoic-Cenozoic tectonic evolution of the Longmen Shan thrust belt, eastern Tibetan Plateau. Tectonics 30, 1–24.
Yang, J.H., Cawood, P.A., Du, Y.S., 2010. Detrital record of mountain building: Provenance of Jurassic foreland basin to the Dabie Mountains. Tectonics 29, 1–19.
Yokoyama, M., Liu, Y., Halim, N., Otofuji, Y., 2001. Paleomagnetic study Of Upper Jurassic rocks from the Sichuan basin: tectonic aspects for the collision between the Yangtze block and North China block. Earth Planet Sci. Lett. 193, 273–285.
Yuan, H.L., Gao, S., Liu, X.M., Li, H.M., Gunther, D., Wu, F.Y., 2004. Accurate U-Pb age and trace element determinations of zircon by laser ablation-inductively coupled plasma mass spectrometry. Geostand. Geoanal. Res. 28, 353–370.
Zhang, G.W., Guo, A.L., Wang, Y.J., Li, S.Z., Dong, Y.P., Liu, S.F., He, D.F., Cheng, S.Y., Lu, R.K., Yao, A.P., 2013. Tectonics of south China continent and its implications. Sci. China (Ser. D) Earth Sci. 56, 1804–1828 (in Chinese with English abstract).
Zhang, G.W., Zhang, B.R., Yuan, X.C., Xiao, Q.H., 2001. Qinling Orogenic Belt and Continental Dynamics. Science Press, Beijing, pp. 1–855.
Zhang, S.B., Zheng, Y.F., Wu, Y.B., Zhao, Z.F., Gao, S., Wu, F.Y., 2006. Zircon U-Pb age and Hf isotope evidence for 3.8Ga crustal remnant and episodic reworking of Archean crust in south China. Earth Planet. Sci. Lett. 252, 56–71.
Zhao, X., Coe, R.S., 1987. Paleomagnetic constraints on collision and rotation of North and South China. Nature 327, 141–144.
Zhou, D.W., Zhang, C.L., Liu, L., Wang, J.L., Liu, Y.Y., 1998. Sm-Nd dating of basic dykes from Wudang block and a discussion of related questions. Acta Geosci. Sinica 19, 25–30 (in Chinese with English abstract).
Zhu, G., Liu, G., Niu, M., Xie, C.L., Wang, Y.S., Xiang, B.W., 2009. Syn-collisional transform faulting of the Tan-Lu fault zone, central China. Int. J. Earth Sci. 98, 135–155.
Zhu, L.M., Zhang, G.W., Chen, Y.J., Ding, Z.J., Guo, B., Wang, F., Lee, B., 2011. Zircon U-Pb ages and geochemistry of the Wenquan Mo-bearing granitioids in West Qinling, China: constraints on the geodynamic setting for the newly discovered Wenquan Mo deposit. Ore Geol. Rev. 39, 46–62.